ACS chemical biology

Articles

pubs.acs.org/acschemicalbiology

N-Myristoyltransferase Is a Cell Wall Target in *Aspergillus fumigatus*

Wenxia Fang,[†] David A. Robinson,[‡] Olawale G. Raimi,[†] David E. Blair,[†] Justin R. Harrison,[‡] Deborah E. A. Lockhart,[†] Leah S. Torrie,[‡] Gian Filippo Ruda,[‡] Paul G. Wyatt,[‡] Ian H. Gilbert,[‡] and Daan M. F. van Aalten*[,†,§]

[†]Division of Molecular Microbiology, [‡]Division of Biological Chemistry and Drug Discovery, [§]MRC Protein Phosphorylation and Ubiquitylation Unit, College of Life Sciences, University of Dundee, Dundee, DD1 5EH, United Kingdom

Supporting Information

ABSTRACT: Treatment of filamentous fungal infections relies on a limited repertoire of antifungal agents. Compounds possessing novel modes of action are urgently required. *N*-myristoylation is a ubiquitous modification of eukaryotic proteins. The enzyme *N*-myristoyltransferase (NMT) has been considered a potential therapeutic target in protozoa and yeasts. Here, we show that the filamentous fungal pathogen *Aspergillus fumigatus* possesses an active NMT enzyme that is essential for survival. Surprisingly, partial repression of the gene revealed downstream effects of *N*-myristoylation on cell wall morphology. Screening a library of inhibitors led to the discovery of a pyrazole sulphonamide compound that inhibits the enzyme and is fungicidal under partially repressive *nmt* conditions. Together with a crystallographic complex showing the inhibitor binding in the peptide substrate pocket, we provide evidence of NMT being a potential drug target in *A. fumigatus*.

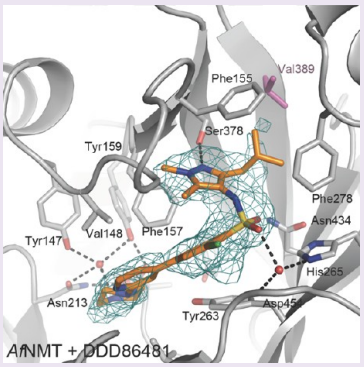

Aspergillus spp. are ubiquitous filamentous fungi and together with three other genera (*Candida*, *Cryptococcus*, and *Pneumocystis*) account for more than 90% of invasive fungal infections worldwide.[1] While invasive aspergillosis due to *A. fumigatus* is estimated to affect over 200 000 people globally each year, a further 3 million are affected by chronic pulmonary aspergillosis.[1] At present, treatment is limited to three antifungal classes: polyenes, azoles, and echinocandins. Voriconazole, introduced in the 1990s, is a third generation azole and current "gold standard" for invasive disease and has increased response and survival rates by 15−20%.[2] Overall mortality for invasive disease, however, remains unacceptable at around 50%.[1] Moreover, there are inherent problems with drug interactions, toxicities, and increasingly reported resistant strains[3,4] necessitating the urgent identification and characterization of novel targets against *A. fumigatus*.

The myristoyl coenzyme A (MCoA)/protein *N*-myristoyltransferase (NMT, EC: 2.3.1.97) catalyzes an irreversible co- and post-translational covalent attachment of the saturated 14-carbon fatty acid, myristate, from MCoA to the *N*-terminal glycine residue of many eukaryotic and viral proteins.[5] *N*-myristoylation is abundant in eukaryotic organisms including protozoa, fungi, and mammals. Membrane targeting and the function of many proteins in a variety of signal transduction cascades and other critical cellular functions is NMT dependent.[5−7] Structural studies advocate an ordered Bi−Bi reaction mechanism[8] whereby binding of MCoA to NMT opens a "lid" permitting access to the peptide-binding site. While the MCoA binding site is highly conserved, NMTs are striking in their remarkable diversity of peptide substrates.[9] Diversity in the peptide-binding groove has been suggested to offer the potential of developing species-specific inhibitors.[9] As a result, NMT has been considered as a potential anticancer,[10] antiviral,[11] and antiparasitic[12−14] therapeutic target. A substantial pool of new chemical starting points for inhibitors of NMTs from parasites has recently been described.[15−21] So far, NMT in filamentous fungi such as *A. fumigatus* remains uncharacterized although orthologues in other fungal pathogens such as *Candida albicans*[22] and *Cryptococcus neoformans*[23] are essential for viability. An NMT knockout in *C. albicans* resulted in avirulence in a murine model,[22] and several prototype inhibitors have been reported.[24−26] Attempts to develop broad-spectrum antifungal NMT inhibitors were unsuccessful and are now potentially redundant given impending improved diagnostics and a developing preference for targeted narrow spectrum therapy.

At present, there is a dearth of new antifungals in the drug discovery pipeline. Conclusive validation of novel antifungal targets from both a chemical and genetic perspective provides a critical first step in reversing this trend. Here, we show that NMT is a potential drug target in *A. fumigatus*.

RESULTS AND DISCUSSION

A. fumigatus Possesses an Active NMT Enzyme. In previous reports, BLAST searches using the *Arabidopsis thaliana* NMT1[27] or *Aspergillus nidulans* NMT[28] sequences predicted the presence of an *nmt* gene (AFUA_4G08070) in the *A. fumigatus* genome. The gene is 1630 bp in length and

Received: October 23, 2014
Accepted: February 23, 2015
Published: February 23, 2015

DOI: 10.1021/cb5008647
ACS Chem. Biol. 2015, 10, 1425−1434

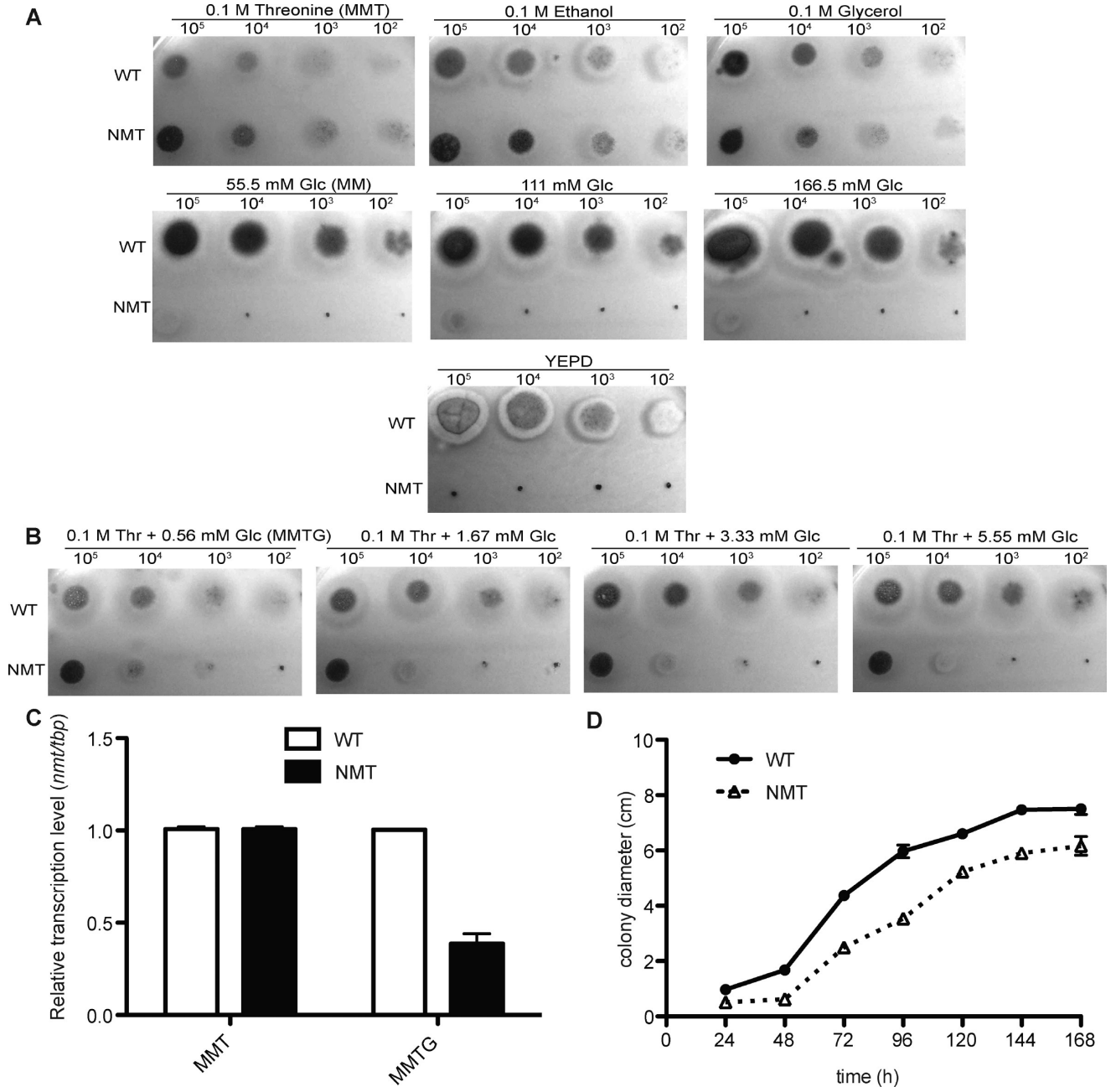

Figure 1. Growth phenotype of the NMT strain under varying repressive conditions. (A) Growth of *A. fumigatus* strains on solid MM supplemented with 0.1 M glycerol, 0.1 M ethanol, 0.1 M threonine or 55.5 mM, 111 mM, 166.5 mM glucose or YEPD. (B) Growth on solid MM supplemented with 0.1 M threonine and 0.56 mM, 1.67 mM 3.33 mM, or 5.55 mM glucose. (C) Real time PCR to amplify the *tbp* and *nmt* gene from MMT and MMTG conditions. (D) Growth curve of the WT and NMT strain on MMTG plates.

contains two introns and three exons. The 1479 bp mRNA encodes a protein of 492 amino acids (UniProt: Q9UVX3) sharing 50%, 52%, 38%, and 44% sequence identity with the NMTs of *C. albicans*, *S. cerevisiae*, *Leishmania major*, and *Homo sapiens* (Supporting Information Figure 1), respectively.

Alignment of *A. fumigatus* NMT (*Af*NMT) with NMT structures deposited in the Protein Data Bank (PDB) from *C. albicans* (1IYL[29]) suggested truncation of the *N*-terminal end, leaving the core catalytic domain intact. Therefore, to increase the chance of crystallization, the first 85 amino acids were removed and a truncated *Af*NMT construct (Δ1−85) generated covering residues 86−492. *Af*NMT Δ1−85 was overexpressed as a GST fusion protein in *Escherichia coli*, purified to homogeneity by glutathione sepharose affinity chromatography followed by proteolysis of the fusion protein and size-exclusion chromatography, yielding 2 mg of pure *Af*NMT per liter of bacterial culture.

*Af*NMT steady-state kinetics were assessed by a scintillation proximity assay [SPA[30,31]] using biotin-tagged cytoskeleton-associated protein 5.5 (CAP5.5) as the peptide acceptor substrate. The K_m of myristoyl-CoA (MCoA) for *Af*NMT was 0.8 ± 0.1 μM (Supporting Information Figure 2A) and comparable to the K_m of MCoA previously reported for *S. cerevisiae* [1.4 μM[32]], *L. major* [1.4 ± 0.3 μM[30]], and *Trypanosoma brucei* [1.8 ± 0.4 μM[30]]. Likewise, the K_m of

DOI: 10.1021/cb5008647
ACS Chem. Biol. 2015, 10, 1425−1434

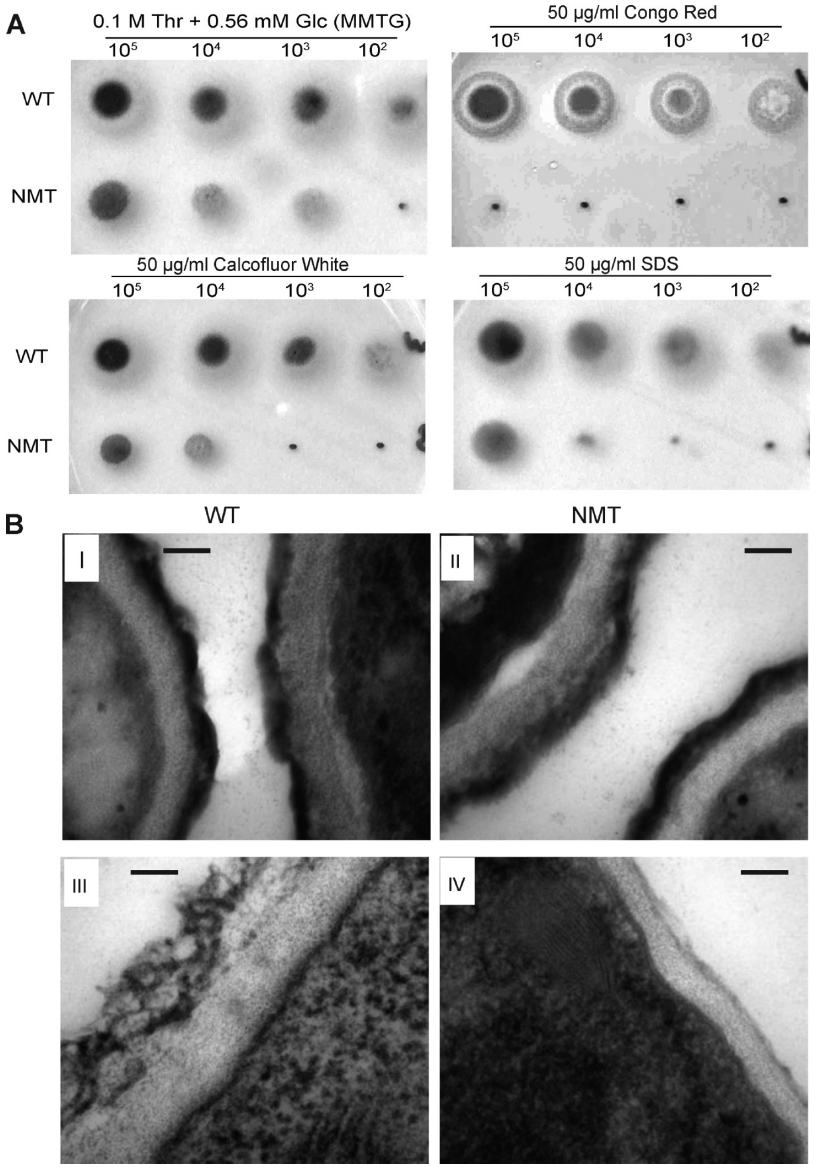

Figure 2. NMT strain sensitivity to chemical reagents and reduction in cell wall thickness. (A) Serial dilutions of conidia from 10^5 to 10^2 were spotted on solid MMTG containing 50 μg mL^{-1} Calcofluor white, Congo red, or SDS. (B) Cell wall architecture under repressive conditions (MMTG). I and II are conidia; III and IV are mycelium. Scale bar is 100 nm.

peptide CAP5.5 for *Af*NMT was 22 ± 2 μM (Supporting Information Figure 2B), similar for *T. brucei* [11 ± 1 μM[30]].

***nmt* Is Essential for Viability of *A. fumigatus*.** Attempts to construct a deletion mutant by replacing the *A. fumigatus* *nmt* gene with a *pyr*G selection marker[33] and phenotypic rescue by supplementing the culture medium with myristic acid failed. Although myristic acid has fully or partially restored the phenotype in other species where *nmt* is essential,[22,23,28] all our transformants failed initial screening with this approach. Instead, a conditional inactivation mutant was constructed by replacing the native promoter of the *nmt* gene with the *A. nidulans* alcohol dehydrogenase promoter (P_{alcA}) that is inducible by ethanol, glycerol, or threonine but repressed by glucose.[34] A plasmid containing a 3′ truncation of *nmt* fused to P_{alcA} was transformed into *A. fumigatus* KU80ΔpyrG$^-$ to generate a conditional mutant (from hereon referred to as the NMT strain) by homologous recombination (Supporting Information Figure 3A). PCR and Southern blotting (Supporting Information Figure 3B–D) verified that in the NMT strain, the inducible P_{alcA} promoter replaced the native promoter of the *nmt* gene.

Growth of the NMT strain was comparable to the WT when grown under conditions of *nmt* induction on a solid minimal medium (MM) containing 0.1 M glycerol, 0.1 M ethanol, or 0.1 M threonine (MMT). However, growth of the NMT strain was completely inhibited under conditions of *nmt* repression on YEPD or MM containing 55.5–166.5 mM glucose after 48 h at 37 °C (Figure 1A). Thus, *nmt* expression is required for viability and is an essential gene in *A. fumigatus*.

***nmt* Expression Affects *A. fumigatus* Cell Wall.** In order to investigate the function of the essential *nmt* gene in *A. fumigatus*, various concentrations of threonine (inducer) and glucose (repressor) were assessed to identify a minimal level of *nmt* expression still producing sufficient mycelia for analysis (Figure 1B). MM with 0.1 M threonine and 0.56 mM glucose (MMTG) was selected for all subsequent phenotypic analysis. Under this condition, the transcription of *nmt* in the NMT strain was reduced to 39% of the WT (Figure 1C). Growth of

DOI: 10.1021/cb5008647
ACS Chem. Biol. 2015, 10, 1425–1434

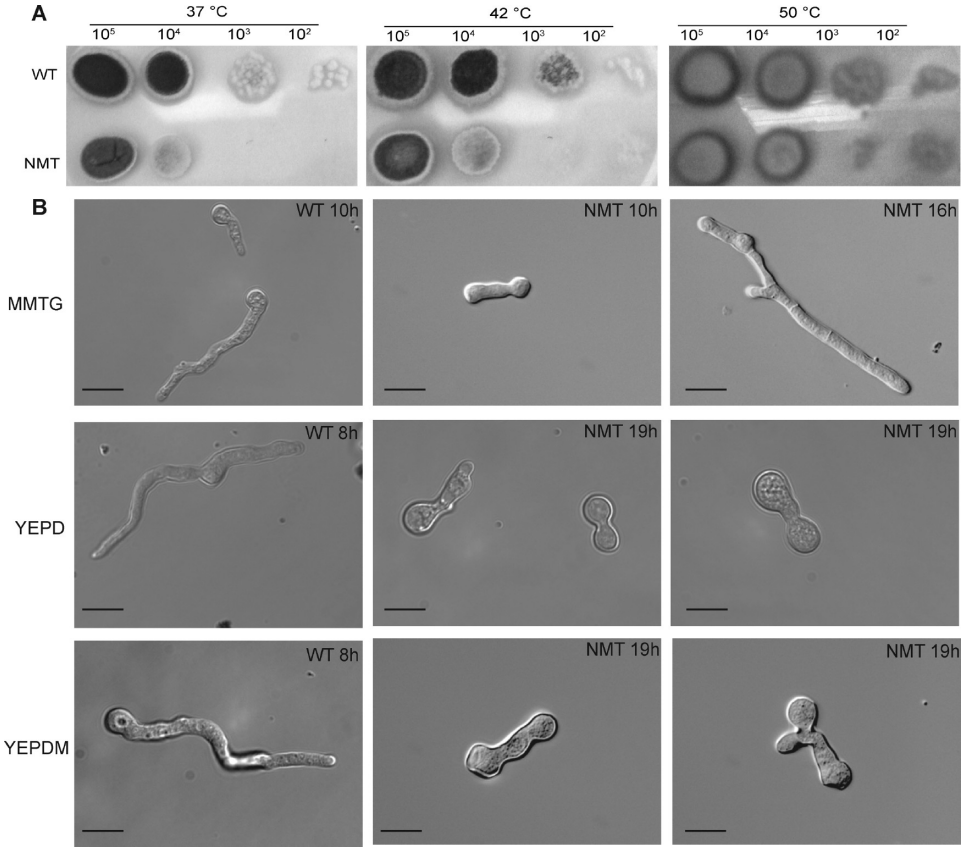

Figure 3. NMT strain temperature insensitivity and delayed germination. (A) Serial dilutions of 10^5 to 10^2 conidia were spotted on MMTG plates and incubated at 37 °C for 36 or 42 h and 50 °C for 60 h before imaging. (B) Comparison of germination times of the WT and NMT strains in MMTG, YEPD, or YEPD supplemented with myristic acid (YEPDM). Scale bar is 10 μm.

the NMT strain was retarded compared to the WT (Figure 1D).

Surprisingly, increased sensitivity to agents compromising the cell wall (Congo red and Calcofluor white) or membrane (Sodium dodecyl sulfate) were observed under partial expression of the *nmt* gene indicative of cell wall defects and loss of membrane integrity (Figure 2A). Furthermore, examination of the cell wall ultrastructure by electron microscopy showed that the conidia of both NMT and WT strains were indistinguishable (Figure 2B, I and II), but the hyphal cell wall of the NMT strain was thinner than the WT (Figure 2B, III and IV).

***nmt* Is Required for Cell Wall Morphogenesis.** Unlike other fungi such as *A. nidulans*[28] where NMT mutants grew only at 37 °C, growth of the NMT strain was unaffected by temperature (37−50 °C) on MMTG plates (Figure 3A). This suggests that the target proteins of *Af*NMT appear to be neither temperature sensitive nor involved in temperature adaptation mechanisms.

Polarized hyphal growth is essential in filamentous fungi and thought to be important for pathogenesis. Our NMT strain showed a marked polar growth defect under conditions of *nmt* repression including delayed germination, abnormal development, and retention of polarity (Figure 3B). When *nmt* was completely repressed in a YEPD medium, the conidia remained swollen or displayed very short germ tubes (Figure 3B), indicating NMT is required for germination and hyphal growth.

Distinct to *A. fumigatus* was the inability of myristic acid supplementation to fully restore the NMT strain to the WT phenotype as has been demonstrated for *C. albicans*, *S. cerevisiae*, and *C. neoformans*.[22,23,35] Only short germ tubes with a ballooned tip or abnormal polarity were evident after 19 h incubation in supplementation medium (Figure 3B).

***Af*NMT Crystal Structure Reveals a Molecular Handle on Selectivity.** As a first step toward the design of selective inhibitors, we determined the crystal structure of *Af*NMT and compared it to the human enzyme. The purified *Af*NMT was cocrystallized with MCoA and the benzofuran compound Ro-09-4879 that is known to compete for peptide binding in other NMTs.[29] The structure of the inhibitor complex was solved by molecular replacement using *C. albicans* NMT (PDB: 1IYK[29]) as a search model and refined against 1.9 Å synchrotron diffraction data (Supporting Information Table 1). No interpretable electron density was visible for the first 15 residues of the polypeptide chain.

The overall crystal structure of *Af*NMT consisted of a monomer of 391 residues (101−492) forming two GCN5 folds with MCoA bound to *Af*NMT in a horseshoe conformation (Figure 4A). To date, crystal structures of NMT from *C. albicans*, *S. cerevisiae*, *H. sapiens*, *L. major*, *L. donovani*, and *P. vivax* have been elucidated showing extensive conservation of the core fold and active site residues (Figure 4B). The structure of *Af*NMT reflects the high level of conservation between species at a primary, secondary, and tertiary sequence level, showing the highest level of conservation with *C. albicans* (Cα RMSD = 1.301 Å with 346 atoms matched) and *S. cerevisiae* NMT (Cα RMSD = 0.840 Å with 350 atoms matched). Although similar to NMT:MCoA structures previously

DOI: 10.1021/cb5008647
ACS Chem. Biol. 2015, 10, 1425−1434

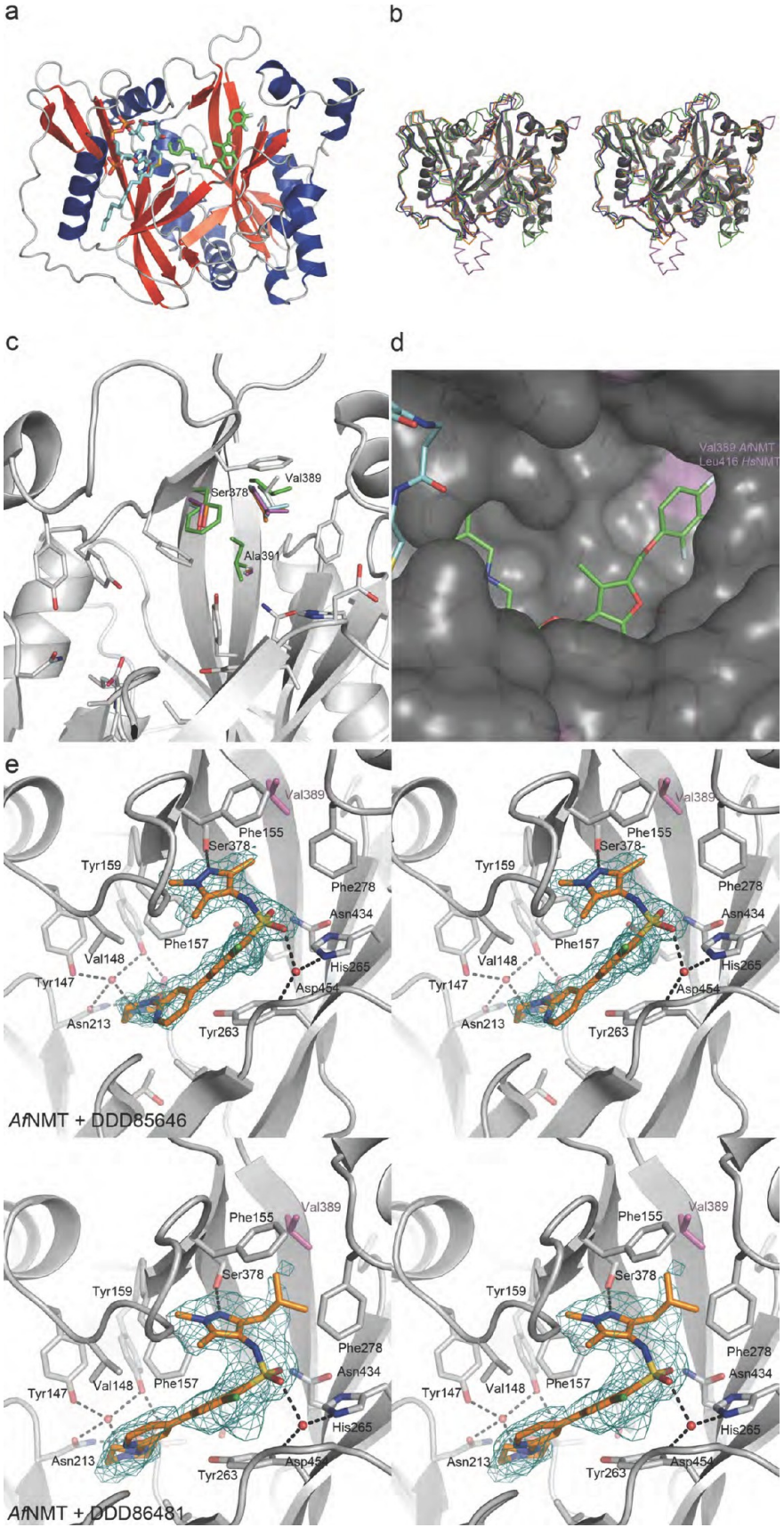

Figure 4. Crystal structure of *Af*NMT complexes with inhibitors. (A) Overall fold of *Af*NMT (residues 86−492) in complex with MCoA (stick representation, C_α cyan) and RO-09-4879 (stick representation, C_α green). (B) Representative crystal structures of NMTs. *Af*NMT shown in gray cartoon superimposed upon *Sc*NMT (PDB 1IIC, green), *Lm*NMT (PDB 3H5Z, magenta), *Hs*NMT1 (PDB 3IU1, cyan), and *Pv*NMT (PDB 4B10, orange). (C) Conservation of NMT active site residues. *Af*NMT backbone shown in gray cartoon with active site side chains shown in stick

DOI: 10.1021/cb5008647
ACS Chem. Biol. 2015, 10, 1425−1434

Figure 4. continued

representation (C atoms gray). Strictly conserved residues between species are shown for *Af*NMT only. Where residues are not conserved, they are shown for all species in stick representation, *Sc*NMT (green), *Lm*NMT (magenta), *Hs*NMT1 (cyan), and *Pv*NMT (orange). (D) Close-up view of the *Af*NMT active site, showing the MCoA (C_α cyan) and RO-09-4879 (C_α green). A molecular surface is shown, colored by sequence conservation with *Hs*NMT1 (gray, identical side chains; purple, nonidentical side chains). (E) Stereoscopic view of the active site of the *Af*NMT in complex with DDD85646 and DDD86481. Active site side chains are shown as sticks with gray C_α, whereas the compound is shown as sticks with gold C_α. The unbiased $|F_o| - |F_c|$ map (2.5 σ) is shown as a green mesh.

determined, the CoA phosphate group was not coordinated by the polypeptide due to the truncated construct lacking the YKFW motif. Electron density for the benzofuran ligand Ro-09-4879 was observed in the peptide-binding groove of *Af*NMT where it competes with acceptor substrate binding (Figure 4A). Here, it adopts a similar conformation to a *Ca*NMT:benzofuran complex [PDB 1IYL[29]]. The peptide binding site of NMT is highly conserved with minimal sequence differences between species. However, comparison of the known NMT crystal structures reveals three nonconserved residues; Ser378 and Ala391 are conserved apart from *C. albicans* and *S. cerevisiae* species where the corresponding residues are Phe and Ile. The residue Val389 is unique to *Af*NMT, and it forms part of a hydrophobic pocket with Phe155, Leu273, Phe278, Ser378, and Val432 that accepts the Ro-09-4879 ligand. In other species, notably human, this residue is a larger leucine (Leu416; Figure 4C,D). Such a difference may be exploitable in the design of inhibitors to selectively target *Af*NMT.

Screening-Based Discovery of a Low Nanomolar AfNMT Inhibitor. Pyrazole sulphonamide ligands act as highly potent inhibitors against *T. brucei* NMT (*Tb*NMT).[12] A panel of antitrypanosome NMT inhibitors was screened against recombinant *Af*NMT (Supporting Information Table 2), and the fungicidal effect on *A. fumigatus* was determined. As shown in Figure 5, two potent nanomolar pyrazole sulphonamide inhibitors were identified using the SPA assay with IC_{50} values of 23 nM (DDD85646) and 12 nM (DDD86481).

To investigate the binding mode of these compounds, further crystal structures of *Af*NMT:MCoA in complex with the pyrazole sulphonamide inhibitors were solved (Supporting Information Table 1), demonstrating that they also occupied the peptide binding site. DDD85646 adopted a similar conformation to that previously observed in a *L. major* NMT complex (PDB 2WSA) used as a model for *T. brucei*.[12] Specifically, the piperazine group interacts with the C-terminal carboxylate group via two bridging water molecules. The first water molecule is tightly coordinated by the C-terminal carboxylate and the phenolic hydroxyl groups of Tyr147 and Tyr159 while a second water molecule bridges the piperazine group and the carboxylate (Figure 4E). The biaryl system makes no specific interactions with the protein and sits on a hydrophobic surface formed by the side chains of Tyr263 and Leu457. A significant bend in the molecule introduced by the sulphonamide allows the pyrazole moiety to penetrate a hydrophobic pocket. Oxygen atoms of the sulphonamide interact with the protein through water-bridged interactions with the side chains of Asn434, His265, and the backbone amides of Asp454 and Gly455. The trimethyl pyrazole group sits in the same hydrophobic pocket occupied by the trifluorophenyl group of Ro-09-4897; however the pyrazole forms a hydrogen bond with the side chain of Ser378 in addition to strong hydrophobic packing interactions (Figure 4E).

The isobutyl pyrazole derivative DDD86481 has a very similar binding mode to DDD85646 (Figure 4E). The

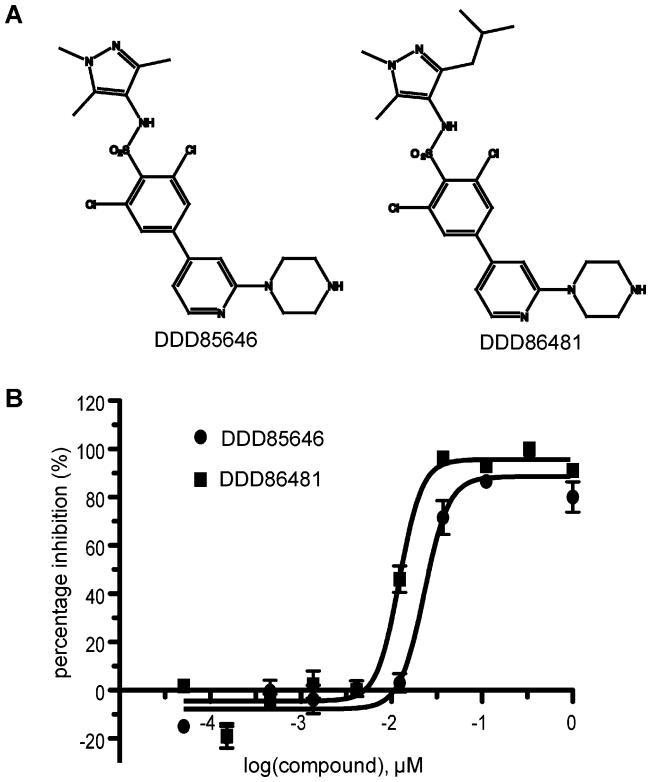

Figure 5. Inhibition of *Af*NMT. (A) Chemical structures of compounds DDD85646 and DDD86481. (B) Dose response IC_{50} curves of DDD85646 and DDD86481 against *Af*NMT using an SPA assay.

sulphonamide, however, sits lower in the active site losing interaction with Asn434, and the pyrazole group rotates slightly to accommodate the larger moiety at the 3- position (Figure 4E). As the isobutyl group packs against the side chains of Phe155, Phe278, Val389, Ala391, and Val432, this explains the increased potency over DDD85646 by increasing the hydrophobic complementarity in this pocket.

DDD86481 Is Fungicidal under Repressed *nmt* Expression. Initially, all compounds from Supporting Information Table 2 were taken for MIC determination in RPMI medium containing 0.1 M threonine and 0.56 mM glucose. Only three compounds (DDD86481, DDD90086, and Ro-09-4879) showed potent inhibition for the NMT mutant. The fungicidal activity of DDD85646 was >2.5 mM irrespective of the *A. fumigatus* strain tested (WT or NMT). Although the MIC of DDD86481 was 925 μM against the WT (at 0.625 mM, WT showed a mutant morphogenesis phenotype), it decreased to 116 μM for the NMT strain (Table 1). As this molecule is more lipophilic than DDD85646, this might account for marginally increased cell penetration and a lower MIC. In order to demonstrate target engagement inside the cell, the chemical labeling technology employing click

DOI: 10.1021/cb5008647
ACS Chem. Biol. 2015, 10, 1425−1434

Table 1. MIC of Inhibitor Compounds against *A. fumigatus*[a]

strains		WT	NMT			
growth conditions	BMT +	0.56 mM Glc	0.56 mM Glc	3.33 mM Glc	55.5 mM Glc	111 mM Glc
level of NMT repression	*nmt* transcription (%)	100 ± 4	81 ± 10	78 ± 15	29 ± 7	24 ± 1
MIC (mM)	DDD86481	0.925	0.116	0.058	0.014	0.007
	DDD85646	>2.5	>2.5	ND	>2.5	>2.5
	DDD90086	>2.5	1.25	ND	0.625	0.625
	Ro-09-4609	>2.5	>2.5	ND	>2.5	>2.5
	Ro-09-4879	0.625	0.625	ND	0.625	0.625
	other compounds*	>2.5	>2.5	ND	ND	ND
	amphotericin B	0.0017	0.0017	0.0017	0.0017	0.0017

[a]The CLSI broth microdilution method was used to determine the MIC (lowest concentration that completely inhibited growth) after 48 h of incubation at 37 °C. BMT, basic medium plus 0.1 M threonine; Glc, glucose; ND, not determined; *All other compounds listed in the Supporting Information, Table 2.

chemistry with a myristate alkyne derivative[13,16,36] was explored. However, this approach did not work in *A. fumigatus* cells, probably because the myristate derivative could not penetrate the fungal cell wall.

To investigate whether DDD86481 was acting through inhibition of *Af*NMT in the NMT strain, MIC values were determined under different repressive conditions and *nmt* transcript levels assessed by quantitative real time PCR. In 0.56 mM glucose medium, *nmt* transcription was 81% of the WT. As *nmt* transcription reduced, DDD86481 efficacy increased with correlating reductions in MIC (Table 1) to 7 μM with 24% *nmt* expression. As a control, the MICs of amphotericin B, DDD85646, Ro-09-4609, and Ro-09-4879 were unaffected by *nmt* transcript levels (Table 1), although the MIC of DDD90086 was decreased slightly. Nevertheless, there is still a significant drop in activity of DDD86481 on going from enzyme to cell. When NMT is normally expressed, there is an 80 000-fold drop in activity; when NMT is expressed at 24%, there is a 600-fold drop in activity. This could be due to poor penetration of DDD86481 through the fungal cell wall but alternatively could be due to the catalytic role of NMT not being essential or off-target effects of DDD86481.

Concluding Remarks. Early stage drug discovery suffers high attrition rates, and there are limited immediate offerings in the antifungal pipeline besides modifications of existing classes.[37] Increased recognition of the clinical burden posed by chronic pulmonary aspergillosis threatens to place huge selective pressures on oral azoles (e.g., itraconazole) as they have been shown to partially alleviate symptoms.[38] Consequently, there is profound medical need for alternative classes ideally with oral formulations. As a step toward this, we presented evidence that validates *Af*NMT as a potential drug target in *A. fumigatus* showing that protein *N*-myristoylation affects cell morphology and integrity of the cell wall, a structure essential to all pathogenic fungi and absent from the human cell.

A conditional NMT mutant strain showed that this gene was essential and also provided insights into the downstream effects of NMT inhibition on the cell wall of *A. fumigatus*. Reduced expression affected cell morphogenesis and cell wall integrity—effects that have not previously been observed in NMT genetic disruption studies in other organisms. The fungal cell wall is a dynamic three-dimensional structure composed predominantly of polysaccharides. The cell wall involves numerous biosynthetic pathways and hundreds of proteins for its synthesis and remodeling. A significant fraction (typically 0.5%) of eukaryotic proteins are thought to be myristoylated,[27] assisting switching between cytoplasmic and membrane bound states. In fact, using the MYR Predictor (http://mendel.imp.ac.at/myristate/SUPLpredictor.htm), 29 proteins from the *A. fumigatus* proteome are predicted to be myristoylated (Supporting Information Table 3). While most proteins are of unknown function, two classes, namely the G-protein alpha subunits and the ADP-ribosylation factors, are known myristoylation substrates.[39,40] Myristoylation of G protein alpha subunits is required for localization to the plasma membrane and also facilitating formation of a heterotrimer for G protein signaling.[41] As signal transducers, G proteins influence numerous signaling cascades especially activate the cyclic-AMP-dependent PKA pathway[42] that regulates growth, development, stress response, morphogenesis, and virulence in *A. fumigatus*.[43−45] There is also direct evidence that G proteins regulate cell wall carbohydrate composition in both plants and other fungi.[46−49] One of the ADP-ribosylation factors in *A. nidulans*, ArfB, is involved in polarity establishment during isotropic growth and polarity maintenance during hyphal extension.[50] Three ArfB orthologues (Afu3g12080, Afu1g11730, and Afu2g10980) in *A. fumigatus* are predicted to be myristoylated proteins (Supporting Information Table 3). Our NMT strain displayed the same polarized growth defect as the ArfB mutant. In summary, we propose that the G alpha subunits and these ArfB orthologues account for the changes in cell wall and defect in morphogenesis in the NMT strain.

Screening a library of compounds identified a 12 nM *Af*NMT inhibitor (DDD86481) that targeted the peptide binding site and interacted with an amino acid side chain that is different between the fungal and human enzyme. However, this failed to directly correlate with fungicidal activity against *A. fumigatus* (MIC 925 μM). Reducing *nmt* expression sensitized the organism to the inhibitor, reducing the MIC to 7 μM, yet retaining a 600-fold difference between activity on the target *in vitro* and the fungal cell, suggesting the need for more potent and cell-penetrant compounds to pursue full chemical validation.

Essential gene targets like NMT produce a lethal phenotype but a significant challenge will be discovering inhibitors that are highly selective for *A. fumigatus*. The peptide-binding sites of the human and *A. fumigatus* NMTs are exquisitely similar to only a single amino acid difference (Val389 in *Af*NMT and Leu416 in *Hs*NMT1). However, there is evidence from *Tb*NMT inhibitors that a substantial window of selectivity can be derived between *Hs*NMT1 and *Tb*NMT despite highly similar active site structures.[12] Recently, further optimized *Tb*NMT inhibitors not only possessed improved CNS

DOI: 10.1021/cb5008647
ACS Chem. Biol. 2015, 10, 1425−1434

penetrance but also improved selectivity that could be used to treat stage 2 human African trypanosomiasis.[21] Highly potent Leishmania-selective NMT inhibitors have been identified either from compound screening[15] or with a structure-based approach.[20] More encouragingly, although structure−activity relationships (SARs) between *Plasmodium* NMT and *Hs*NMT1 overlap,[15] potent and selective *Plasmodium* NMT inhibitors have been discovered[15] and optimized,[18] demonstrating that even the small conformational differences of single equivalent tyrosine could be exploited to engineer selectivity over the human enzyme.[17] Therefore, it may be possible to discover selective *A. fumigatus* inhibitors based on the structure differences between *Af*NMT and *Hs*NMT1 described here.

In summary, we have provided the first comprehensive characterization of NMT in a filamentous fungal pathogen and combined genetic, structural, and chemical approaches to validate *Af*NMT as a target illustrating NMT dependent inhibition of *A. fumigatus* growth. While the genetic work confirmed NMT is essential for viability in *A. fumigatus*, the mutant NMT strain allows controlled gene expression and provides a research tool for further probing the effects of (i) *N*-myristoylation and (ii) host-fungal interactions.

METHODS

Construction of the Conditional Inactivation Mutant. Plasmid pAL3 containing the *A. nidulans alcA* promoter (P_{alcA}) and the *Neurospora crassa pyr-4* gene as a fungal selectable marker[51] was used to construct a vector replacing the native *nmt* promoter with P_{alcA}. An 1120 bp fragment from −50 to +1070 of the *nmt* genomic DNA sequence was amplified with primers P3 and P4 (see Supporting Information Table 4 for all primer sequences) containing a *Kpn*I and *Xba*I restriction site, respectively. The PCR-amplified fragment was cloned into expression vector pAL3 to yield pALnmtN and confirmed by sequencing. The pALnmtN was transformed into *A. fumigatus* strain KU80ΔpyrG$^-$ by PEG-mediated fusion of protoplasts[52] and screened for colonies with uridine/uracil autotrophy. The transformants were confirmed by PCR and Southern blot analysis.

For PCR analysis, three sets of primers were designed: primers P5 and P6 for the 1.6 kb *nmt* gene, P7 and P8 for the 1.2 kb *pyr-4* marker, and P9 and P10 for a 2.5 kb fragment from P_{alcA} to a downstream region of the *nmt* gene. For Southern blotting, genomic DNA was digested with *Bam*HI, separated by electrophoresis and transferred to a nylon membrane (Zeta-probe+, Bio-Rad). The 1120 bp fragment of the *nmt* genomic sequence and a 1.2 kb *Hind*III fragment of the *N. crassa pyr-4* gene from pAL3 were used as probes. Labeling and visualization were performed using the DIG DNA labeling and detection kit (Roche) according to the manufacturer's instructions.

Crystallization, Data Collection, and Structure Determination. *Af*NMT Δ1−85 (20 mg mL^{-1}) was crystallized using the sitting drop method. Prior to crystallization, *Af*NMT was incubated with 10 mM myristoylCoA (MCoA). To obtain ligand complexes, *Af*NMT was incubated with 10 mM of compound. Crystals grew after 2 days in a mother liquor of 0.2 M NaCl and 25% (v/v) PEG3350 and were cryoprotected for flash freezing in liquid nitrogen. Diffraction data were collected at the European Synchrotron Radiation Facility (ESRF, Grenoble, France) and all data processed and scaled with HKL software.[53]

The *Af*NMT-MCoA-RO-09-4879 complex structure was solved by molecular replacement using MOLREP[54] from the CCP4 suite programs[55] with the *C. albicans* NMT structure (PDB: 1IYK[29]) as a search model giving a solution with one molecule in the asymmetric unit. The resulting electron density map was of good quality, allowing WarpNtrace[56] to build virtually all residues except for a few disordered regions. REFMAC5[57] was used for further refinement, iterated with model building using COOT,[58] producing a final model with the statistics shown in Supporting Information Table 1. Other compound complexes were solved by molecular replacement using the *Af*NMT-MCoA-RO-09-4879 structure as a search model. The model for ligands was not included until their conformations were fully defined by unbiased $|F_o| - |F_c|\ \phi_{calc}$ electron density maps. Ligand structures and topologies were generated by PRODRG.[59] PyMol was used to generate figures.[60]

Minimal Inhibitory Concentration (MIC) Assay. Selected compounds were tested against *A. fumigatus* (WT [KU80] and NMT strains) according to the Clinical and Laboratory Standards Institute (CLSI) M38-A broth microdilution methodology.[61] All compounds were dissolved in DMSO, and the final DMSO concentration was 2.5% (v/v) in all wells. The MIC end point was defined as the lowest concentration producing complete inhibition of growth (MIC_{100}) for all compounds studied. The MIC values for each compound were determined in triplicate. Amphotericin B (Sigma) and *A. fumigatus* ATCC 204305 served as a positive control and the MIC within the recommended limits of CLSI M38-A.

ASSOCIATED CONTENT

Supporting Information

Supporting Figures S1−S3, Supporting Tables S1−S4, and further details of experimental procedures. This material is available free of charge via the Internet from http://pubs.acs.org.

Accession Codes

The atomic coordinates and structure factors of *Af*NMT:MCoA with RO-09-4879, DDD85646, and DDD86481 have been deposited in the Protein Data Bank with accession codes 4CAV, 4CAX, and 4CAW.

Other procedures are reported in the Supporting Information.

AUTHOR INFORMATION

Corresponding Author

*E-mail: dmfvanaalten@dundee.ac.uk.

Notes

The authors declare no competing financial interest.

ACKNOWLEDGMENTS

The authors would like to thank the European Synchrotron Radiation facility (ESRF), Grenoble, for beamline time. We thank J. James of the College of Life Sciences Microscopy Facility for his help with electron microscopy. We also thank F. Eisenhaber, Bioinformatics Institute Singapore, for predicting myristoylated proteins. This work was funded by an MRC Programme Grant (M004139) and a Wellcome Trust Senior Research Fellowship (WT087590MA) to D.M.F.v.A. D.E.A.L was supported by an MRC Clinical Research Training Fellowship (G1100430). We also would like to acknowledge the Wellcome Trust (WT077705, WT083481) for support.

REFERENCES

(1) Brown, G. D., Denning, D. W., Gow, N. A., Levitz, S. M., Netea, M. G., and White, T. C. (2012) Hidden killers: human fungal infections. *Sci. Transl. Med. 4*, 165rv113.

(2) Nivoix, Y., Velten, M., Letscher-Bru, V., Moghaddam, A., Natarajan-Ame, S., Fohrer, C., Lioure, B., Bilger, K., Lutun, P., Marcellin, L., Launoy, A., Freys, G., Bergerat, J. P., and Herbrecht, R. (2008) Factors associated with overall and attributable mortality in invasive aspergillosis. *Clin. Infect. Dis. 47*, 1176−1184.

(3) Bowyer, P., Moore, C. B., Rautemaa, R., Denning, D. W., and Richardson, M. D. (2011) Azole antifungal resistance today: focus on Aspergillus. *Curr. Infect Dis. Rep. 13*, 485−491.

(4) van der Linden, J. W., Camps, S. M., Kampinga, G. A., Arends, J. P., Debets-Ossenkopp, Y. J., Haas, P. J., Rijnders, B. J., Kuijper, E. J., van Tiel, F. H., Varga, J., Karawajczyk, A., Zoll, J., Melchers, W. J., and

DOI: 10.1021/cb5008647
ACS Chem. Biol. 2015, 10, 1425−1434

Verweij, P. E. (2013) Aspergillosis due to voriconazole highly resistant Aspergillus fumigatus and recovery of genetically related resistant isolates from domiciles. *Clin. Infect. Dis. 57*, 513−520.
(5) Farazi, T. A., Waksman, G., and Gordon, J. I. (2001) The biology and enzymology of protein N-myristoylation. *J. Biol. Chem. 276*, 39501−39504.
(6) Knoll, L. J., Johnson, D. R., Bryant, M. L., and Gordon, J. I. (1995) Functional significance of myristoyl moiety in N-myristoyl proteins. *Methods Enzymol. 250*, 405−435.
(7) Boutin, J. A. (1997) Myristoylation. *Cell. Signal. 9*, 15−35.
(8) Rudnick, D. A., McWherter, C. A., Rocque, W. J., Lennon, P. J., Getman, D. P., and Gordon, J. I. (1991) Kinetic and structural evidence for a sequential ordered Bi Bi mechanism of catalysis by Saccharomyces cerevisiae myristoyl-CoA:protein N-myristoyltransferase. *J. Biol. Chem. 266*, 9732−9739.
(9) Kishore, N. S., Wood, D. C., Mehta, P. P., Wade, A. C., Lu, T., Gokel, G. W., and Gordon, J. I. (1993) Comparison of the acyl chain specificities of human myristoyl-CoA synthetase and human myristoyl-CoA:protein N-myristoyltransferase. *J. Biol. Chem. 268*, 4889−4902.
(10) Selvakumar, P., Lakshmikuttyamma, A., Shrivastav, A., Das, S. B., Dimmock, J. R., and Sharma, R. K. (2007) Potential role of N-myristoyltransferase in cancer. *Prog. Lipid Res. 46*, 1−36.
(11) Hill, B. T., and Skowronski, J. (2005) Human N-myristoyltransferases form stable complexes with lentiviral nef and other viral and cellular substrate proteins. *J. Virol. 79*, 1133−1141.
(12) Frearson, J. A., Brand, S., McElroy, S. P., Cleghorn, L. A., Smid, O., Stojanovski, L., Price, H. P., Guther, M. L., Torrie, L. S., Robinson, D. A., Hallyburton, I., Mpamhanga, C. P., Brannigan, J. A., Wilkinson, A. J., Hodgkinson, M., Hui, R., Qiu, W., Raimi, O. G., van Aalten, D. M., Brenk, R., Gilbert, I. H., Read, K. D., Fairlamb, A. H., Ferguson, M. A., Smith, D. F., and Wyatt, P. G. (2010) N-myristoyltransferase inhibitors as new leads to treat sleeping sickness. *Nature 464*, 728−732.
(13) Wright, M. H., Clough, B., Rackham, M. D., Rangachari, K., Brannigan, J. A., Grainger, M., Moss, D. K., Bottrill, A. R., Heal, W. P., Broncel, M., Serwa, R. A., Brady, D., Mann, D. J., Leatherbarrow, R. J., Tewari, R., Wilkinson, A. J., Holder, A. A., and Tate, E. W. (2014) Validation of N-myristoyltransferase as an antimalarial drug target using an integrated chemical biology approach. *Nat. Chem. 6*, 112−121.
(14) Tate, E. W., Bell, A. S., Rackham, M. D., and Wright, M. H. (2014) N-Myristoyltransferase as a potential drug target in malaria and leishmaniasis. *Parasitology 141*, 37−49.
(15) Bell, A. S., Mills, J. E., Williams, G. P., Brannigan, J. A., Wilkinson, A. J., Parkinson, T., Leatherbarrow, R. J., Tate, E. W., Holder, A. A., and Smith, D. F. (2012) Selective inhibitors of protozoan protein N-myristoyltransferases as starting points for tropical disease medicinal chemistry programs. *PLoS Negl. Trop. Dis. 6*, e1625.
(16) Thinon, E., Serwa, R. A., Broncel, M., Brannigan, J. A., Brassat, U., Wright, M. H., Heal, W. P., Wilkinson, A. J., Mann, D. J., and Tate, E. W. (2014) Global profiling of co- and post-translationally N-myristoylated proteomes in human cells. *Nat. Commun. 5*, 4919.
(17) Yu, Z., Brannigan, J. A., Moss, D. K., Brzozowski, A. M., Wilkinson, A. J., Holder, A. A., Tate, E. W., and Leatherbarrow, R. J. (2012) Design and synthesis of inhibitors of Plasmodium falciparum N-myristoyltransferase, a promising target for antimalarial drug discovery. *J. Med. Chem. 55*, 8879−8890.
(18) Rackham, M. D., Brannigan, J. A., Rangachari, K., Meister, S., Wilkinson, A. J., Holder, A. A., Leatherbarrow, R. J., and Tate, E. W. (2014) Design and synthesis of high affinity inhibitors of Plasmodium falciparum and Plasmodium vivax N-myristoyltransferases directed by ligand efficiency dependent lipophilicity (LELP). *J. Med. Chem. 57*, 2773−2788.
(19) Olaleye, T. O., Brannigan, J. A., Roberts, S. M., Leatherbarrow, R. J., Wilkinson, A. J., and Tate, E. W. (2014) Peptidomimetic inhibitors of N-myristoyltransferase from human malaria and leishmaniasis parasites. *Org. Biomol. Chem. 12*, 8132−8137.
(20) Hutton, J. A., Goncalves, V., Brannigan, J. A., Paape, D., Wright, M. H., Waugh, T. M., Roberts, S. M., Bell, A. S., Wilkinson, A. J., Smith, D. F., Leatherbarrow, R. J., and Tate, E. W. (2014) Structure-based design of potent and selective Leishmania N-myristoyltransferase inhibitors. *J. Med. Chem. 57*, 8664−8670.
(21) Brand, S., Norcross, N. R., Thompson, S., Harrison, J. R., Smith, V. C., Robinson, D. A., Torrie, L. S., McElroy, S. P., Hallyburton, I., Norval, S., Scullion, P., Stojanovski, L., Simeons, F. R., van Aalten, D., Frearson, J. A., Brenk, R., Fairlamb, A. H., Ferguson, M. A., Wyatt, P. G., Gilbert, I. H., and Read, K. D. (2014) Lead optimization of a pyrazole sulfonamide series of Trypanosoma brucei N-myristoyltransferase inhibitors: identification and evaluation of CNS penetrant compounds as potential treatments for stage 2 human African trypanosomiasis. *J. Med. Chem. 57*, 9855−9869.
(22) Weinberg, R. A., McWherter, C. A., Freeman, S. K., Wood, D. C., Gordon, J. I., and Lee, S. C. (1995) Genetic studies reveal that myristoylCoA:protein N-myristoyltransferase is an essential enzyme in Candida albicans. *Mol. Microbiol. 16*, 241−250.
(23) Lodge, J. K., Jackson-Machelski, E., Toffaletti, D. L., Perfect, J. R., and Gordon, J. I. (1994) Targeted gene replacement demonstrates that myristoyl-CoA: protein N-myristoyltransferase is essential for viability of Cryptococcus neoformans. *Proc. Natl. Acad. Sci. U. S. A. 91*, 12008−12012.
(24) Devadas, B., Freeman, S. K., Zupec, M. E., Lu, H. F., Nagarajan, S. R., Kishore, N. S., Lodge, J. K., Kuneman, D. W., McWherter, C. A., Vinjamoori, D. V., Getman, D. P., Gordon, J. I., and Sikorski, J. A. (1997) Design and synthesis of novel imidazole-substituted dipeptide amides as potent and selective inhibitors of Candida albicans myristoylCoA:protein N-myristoyltransferase and identification of related tripeptide inhibitors with mechanism-based antifungal activity. *J. Med. Chem. 40*, 2609−2625.
(25) Masubuchi, M., Kawasaki, K., Ebiike, H., Ikeda, Y., Tsujii, S., Sogabe, S., Fujii, T., Sakata, K., Shiratori, Y., Aoki, Y., Ohtsuka, T., and Shimma, N. (2001) Design and synthesis of novel benzofurans as a new class of antifungal agents targeting fungal N-myristoyltransferase. *Bioorg. Med. Chem. Lett. 11* (Part1), 1833−1837.
(26) Ebiike, H., Masubuchi, M., Liu, P., Kawasaki, K., Morikami, K., Sogabe, S., Hayase, M., Fujii, T., Sakata, K., Shindoh, H., Shiratori, Y., Aoki, Y., Ohtsuka, T., and Shimma, N. (2002) Design and synthesis of novel benzofurans as a new class of antifungal agents targeting fungal N-myristoyltransferase. *Bioorg. Med. Chem. Lett. 12* (Part 2), 607−610.
(27) Maurer-Stroh, S., Eisenhaber, B., and Eisenhaber, F. (2002) N-terminal N-myristoylation of proteins: prediction of substrate proteins from amino acid sequence. *J. Mol. Biol. 317*, 541−557.
(28) Shaw, B. D., Momany, C., and Momany, M. (2002) Aspergillus nidulans swoF encodes an N-myristoyl transferase. *Eukaryot Cell 1*, 241−248.
(29) Sogabe, S., Masubuchi, M., Sakata, K., Fukami, T. A., Morikami, K., Shiratori, Y., Ebiike, H., Kawasaki, K., Aoki, Y., Shimma, N., D'Arcy, A., Winkler, F. K., Banner, D. W., and Ohtsuka, T. (2002) Crystal structures of Candida albicans N-myristoyltransferase with two distinct inhibitors. *Chem. Biol. 9*, 1119−1128.
(30) Panethymitaki, C., Bowyer, P. W., Price, H. P., Leatherbarrow, R. J., Brown, K. A., and Smith, D. F. (2006) Characterization and selective inhibition of myristoyl-CoA:protein N-myristoyltransferase from Trypanosoma brucei and Leishmania major. *Biochem. J. 396*, 277−285.
(31) Bowyer, P. W., Gunaratne, R. S., Grainger, M., Withers-Martinez, C., Wickramsinghe, S. R., Tate, E. W., Leatherbarrow, R. J., Brown, K. A., Holder, A. A., and Smith, D. F. (2007) Molecules incorporating a benzothiazole core scaffold inhibit the N-myristoyltransferase of Plasmodium falciparum. *Biochem. J. 408*, 173−180.
(32) Rocque, W. J., McWherter, C. A., Wood, D. C., and Gordon, J. I. (1993) A comparative analysis of the kinetic mechanism and peptide substrate specificity of human and Saccharomyces cerevisiae myristoyl-CoA:protein N-myristoyltransferase. *J. Biol. Chem. 268*, 9964−9971.
(33) d'Enfert, C. (1996) Selection of multiple disruption events in Aspergillus fumigatus using the orotidine-5′-decarboxylase gene, pyrG, as a unique transformation marker. *Curr. Genet. 30*, 76−82.

DOI: 10.1021/cb5008647
ACS Chem. Biol. 2015, 10, 1425−1434

(34) Romero, B., Turner, G., Olivas, I., Laborda, F., and De Lucas, J. R. (2003) The Aspergillus nidulans alcA promoter drives tightly regulated conditional gene expression in Aspergillus fumigatus permitting validation of essential genes in this human pathogen. *Fungal Genet. Biol. 40*, 103−114.
(35) Duronio, R. J., Rudnick, D. A., Johnson, R. L., Johnson, D. R., and Gordon, J. I. (1991) Myristic acid auxotrophy caused by mutation of S. cerevisiae myristoyl-CoA:protein N-myristoyltransferase. *J. Cell Biol. 113*, 1313−1330.
(36) Heal, W. P., Wright, M. H., Thinon, E., and Tate, E. W. (2012) Multifunctional protein labeling via enzymatic N-terminal tagging and elaboration by click chemistry. *Nat. Protoc. 7*, 105−117.
(37) Howard, S. J., Lass-Florl, C., Cuenca-Estrella, M., Gomez-Lopez, A., and Arendrup, M. C. (2013) Isavuconazole susceptibility of Aspergillus and Candida species by EUCAST method. *Antimicrob. Agents Chemother. 57*, 5426−5431.
(38) Denning, D. W., and Bowyer, P. (2013) Voriconazole resistance in Aspergillus fumigatus: should we be concerned? *Clin. Infect. Dis. 57*, 521−523.
(39) Mumby, S. M., Heukeroth, R. O., Gordon, J. I., and Gilman, A. G. (1990) G-protein alpha-subunit expression, myristoylation, and membrane association in COS cells. *Proc. Natl. Acad. Sci. U. S. A. 87*, 728−732.
(40) Lee, S. C., and Shaw, B. D. (2008) ArfB links protein lipidation and endocytosis to polarized growth of Aspergillus nidulans. *Commun. Integr. Biol. 1*, 51−52.
(41) Linder, M. E., Pang, I. H., Duronio, R. J., Gordon, J. I., Sternweis, P. C., and Gilman, A. G. (1991) Lipid modifications of G protein subunits. Myristoylation of Go alpha increases its affinity for beta gamma. *J. Biol. Chem. 266*, 4654−4659.
(42) Lafon, A., Seo, J. A., Han, K. H., Yu, J. H., and d'Enfert, C. (2005) The heterotrimeric G-protein GanB(alpha)-SfaD(beta)-GpgA-(gamma) is a carbon source sensor involved in early cAMP-dependent germination in Aspergillus nidulans. *Genetics 171*, 71−80.
(43) Liebmann, B., Gattung, S., Jahn, B., and Brakhage, A. A. (2003) cAMP signaling in Aspergillus fumigatus is involved in the regulation of the virulence gene pksP and in defense against killing by macrophages. *Mol. Genet. Genomics 269*, 420−435.
(44) Zhao, W., Panepinto, J. C., Fortwendel, J. R., Fox, L., Oliver, B. G., Askew, D. S., and Rhodes, J. C. (2006) Deletion of the regulatory subunit of protein kinase A in Aspergillus fumigatus alters morphology, sensitivity to oxidative damage, and virulence. *Infect. Immun. 74*, 4865−4874.
(45) Liebmann, B., Muller, M., Braun, A., and Brakhage, A. A. (2004) The cyclic AMP-dependent protein kinase a network regulates development and virulence in Aspergillus fumigatus. *Infect. Immun. 72*, 5193−5203.
(46) Yu, H. Y., Seo, J. A., Kim, J. E., Han, K. H., Shim, W. B., Yun, S. H., and Lee, Y. W. (2008) Functional analyses of heterotrimeric G protein G alpha and G beta subunits in Gibberella zeae. *Microbiology 154*, 392−401.
(47) Klopffleisch, K., Phan, N., Augustin, K., Bayne, R. S., Booker, K. S., Botella, J. R., Carpita, N. C., Carr, T., Chen, J. G., Cooke, T. R., Frick-Cheng, A., Friedman, E. J., Fulk, B., Hahn, M. G., Jiang, K., Jorda, L., Kruppe, L., Liu, C., Lorek, J., McCann, M. C., Molina, A., Moriyama, E. N., Mukhtar, M. S., Mudgil, Y., Pattathil, S., Schwarz, J., Seta, S., Tan, M., Temp, U., Trusov, Y., Urano, D., Welter, B., Yang, J., Panstruga, R., Uhrig, J. F., and Jones, A. M. (2011) Arabidopsis G-protein interactome reveals connections to cell wall carbohydrates and morphogenesis. *Mol. Syst. Biol. 7*, 532.
(48) Delgado-Cerezo, M., Sanchez-Rodriguez, C., Escudero, V., Miedes, E., Fernandez, P. V., Jorda, L., Hernandez-Blanco, C., Sanchez-Vallet, A., Bednarek, P., Schulze-Lefert, P., Somerville, S., Estevez, J. M., Persson, S., and Molina, A. (2012) Arabidopsis heterotrimeric G-protein regulates cell wall defense and resistance to necrotrophic fungi. *Mol. Plant 5*, 98−114.
(49) Coca, M. A., Damsz, B., Yun, D. J., Hasegawa, P. M., Bressan, R. A., and Narasimhan, M. L. (2000) Heterotrimeric G-proteins of a filamentous fungus regulate cell wall composition and susceptibility to a plant PR-5 protein. *Plant J. 22*, 61−69.
(50) Lee, S. C., Schmidtke, S. N., Dangott, L. J., and Shaw, B. D. (2008) Aspergillus nidulans ArfB plays a role in endocytosis and polarized growth. *Eukaryot Cell 7*, 1278−1288.
(51) Waring, R. B., May, G. S., and Morris, N. R. (1989) Characterization of an inducible expression system in Aspergillus nidulans using alcA and tubulin-coding genes. *Gene 79*, 119−130.
(52) Langfelder, K., Gattung, S., and Brakhage, A. A. (2002) A novel method used to delete a new Aspergillus fumigatus ABC transporter-encoding gene. *Curr. Genet. 41*, 268−274.
(53) Otwinowski, Z., and Minor, A. (1997) Processing of X-ray diffraction data collected in oscillation mode. *Methods Enzymol.*, 307−326.
(54) Vagin, A., and Teplyakov, A. (1997) MOLREP: an automated program for molecular replacement. *J. Appl. Crystallogr. 30*, 1022−1025.
(55) (1994) The CCP4 suite: programs for protein crystallography, *Acta Crystallogr., Sect. D: Biol. Crystallogr. 50*, 760−763.
(56) Perrakis, A., Morris, R., and Lamzin, V. S. (1999) Automated protein model building combined with iterative structure refinement. *Nat. Struct. Biol. 6*, 458−463.
(57) Murshudov, G. N., Vagin, A. A., and Dodson, E. J. (1997) Refinement of macromolecular structures by the maximum-likelihood method. *Acta Crystallogr., Sect. D: Biol. Crystallogr. 53*, 240−255.
(58) Emsley, P., and Cowtan, K. (2004) Coot: model-building tools for molecular graphics. *Acta Crystallogr., Sect. D: Biol. Crystallogr. 60*, 2126−2132.
(59) Schuettelkopf, A. W., and van Aalten, D. M. F. (2004) PRODRG: a tool for high-throughput crystallography of protein-ligand complexes. *Acta Crystallogr., Sect. D: Biol. Crystallogr. 60*, 1355−1363.
(60) DeLano, W. L. (2004) Use of PYMOL as a communication tool for molecular science. *Abstr. Pap. Am. Chem. Soc. 228*, 030-CHED.
(61) Espinel-Ingroff, A., Fothergill, A., Ghannoum, M., Manavathu, E., Ostrosky-Zeichner, L., Pfaller, M. A., Rinaldi, M. G., Schell, W., and Walsh, T. J. (2007) Quality control and reference guidelines for CLSI broth microdilution method (M38-A document) for susceptibility testing of anidulafungin against molds. *J. Clin. Microbiol. 45*, 2180−2182.

DOI: 10.1021/cb5008647
ACS Chem. Biol. 2015, 10, 1425−1434